Chemistry & Biology
Article

Molecular Analysis of the Kirromycin Biosynthetic Gene Cluster Revealed β-Alanine as Precursor of the Pyridone Moiety

Tilmann Weber,[1,*] Kristina Juliane Laiple,[1] Eva Karoline Pross,[1] Adriana Textor,[2] Stephanie Grond,[2] Katrin Welzel,[3] Stefan Pelzer,[3] Andreas Vente,[3] and Wolfgang Wohlleben[1]
[1]Eberhard-Karls-Universität Tübingen, Fakultät für Biologie, Mikrobiologie/Biotechnologie, Auf der Morgenstelle 28, 72076 Tübingen, Germany
[2]Georg-August-Universität Göttingen, Institut für Organische und Biomolekulare Chemie, Tammannstr. 2, 37077 Göttingen, Germany
[3]Combinature Biopharm AG, Robert-Rössle-Strasse 10, 13125 Berlin, Germany
*Correspondence: tilmann.weber@biotech.uni-tuebingen.de
DOI 10.1016/j.chembiol.2007.12.009

SUMMARY

Kirromycin is a complex linear polyketide that acts as a protein biosynthesis inhibitor by binding to the bacterial elongation factor Tu. The kirromycin biosynthetic gene cluster was isolated from the producer, *Streptomyces collinus* Tü 365, and confirmed by targeted disruption of essential biosynthesis genes. Kirromycin is synthesized by a large hybrid polyketide synthase (PKS)/nonribosomal peptide synthetase (NRPS) encoded by the genes *kirAI–kirAVI*. This complex involves some very unusual features, including the absence of internal acyltransferase (AT) domains in KirAI-KirAV, multiple split-ups of PKS modules on separate genes, and swapping in the domain organization. Interestingly, one PKS enzyme, KirAVI, contains internal AT domains. Based on in silico analysis, a route to pyridone formation involving PKS and NRPS steps was postulated. This hypothesis was experimentally proven by feeding studies with [U-$^{13}C_3$ ^{15}N]β-alanine and NMR and MS analyses of the isolated pure kirromycin.

INTRODUCTION

Wolf and Zähner (1972) first isolated kirromycin from the actinomycete, *Streptomyces collinus* Tü 365, in a screening program for narrow-spectrum antibiotics. Around that time, Vos and Verwiel isolated a compound named mocimycin, which is identical to kirromycin (delvomycin, demethylaurodox) (Vos and Verwiel, 1973; Maehr et al., 1973). Other microbial natural products are structurally related to kirromycin, such as aurodox (Berger et al., 1973), kirrothricin (Thein-Schranner et al., 1982), efrotomycin (Wax et al., 1976), ganefromycin (Carter et al., 1988), and heneicomycin (Zimmerman et al., 1979).

The biological target for kirromycin was elucidated soon after its discovery. Kirromycin interacts specifically with the bacterial elongation factor Tu (EF-Tu) (Wolf et al., 1972; Wolf et al., 1974; for a comprehensive review, see Parmeggiani and Swart, 1985), a rare target for antibiotics. Hence, the name elfamycins comprises the group of active kirromycin and its congeners.

Cocrystallization of aurodox (*N*-methyl kirromycin) with purified EF-Tu from *Thermus aquaticus* revealed that the substance binds to the interface of domains I and II of the EF-Tu (Vogeley et al., 2001). This binding results in a protein conformation that is no longer able to dissociate from the ribosome, which leads to a stalling of the ribosome. Additionally, kirromycin binding alters many intrinsic properties of its target: an interaction of EF-Tu with kirromycin results in stimulation of GTPase activity, a decreased affinity of the ternary complex to bind aminoacyl-tRNA, a failure to interact with EF-Tu, an increased nucleotide exchange rate for GDP, an increased affinity toward GTP, and the abolishment of EF-Tu phosphorylation (Alexander et al., 1995). This target makes kirromycin and its derivatives important tools in protein biosynthesis research as well as interesting candidates for drug development.

Previous studies proved that kirromycin has strong activity against *Streptococci* and some *Enterococci* strains, *Neisseria gonorrhoeae* and *Haemophilus influenzae* (Tavecchia et al., 1996), whereas, for example, the EF-Tu of *Staphylococcus aureus* is intrinsically resistant to the antibiotic (Hall et al., 1989). This restricted spectrum of antimicrobial activity is different from many other antibiotics, where clear biases toward gram-positive or gram-negative bacteria can be observed. Although there were no toxic effects observed on higher eukaryotic cells (Schmid et al., 1978), kirromycin is active against blood cultures of the malaria parasite, *Plasmodium falciparum*, by interfering with organelle-based protein biosynthesis. (Clough et al., 1999).

Two main causes are known to account for the narrow susceptibility range of kirromycin in the tested organisms: mutations around the kirromycin binding site in EF-Tu gene can lead to proteins that are resistant to the antibiotic, but retain full functionality in the protein biosynthesis process (e.g., Mesters et al., 1994); in other cases, it has been suggested that kirromycin and related compounds cannot permeate into the cells or are exported before interaction with EF-Tu.

Unexpectedly, *S. collinus* Tü 365, the kirromycin producer, and *S. ramocissimus*, the mocimycin producer, both express kirromycin-sensitive elongation factors, also during antibiotic production (Olsthoorn-Tieleman et al., 2007). These strains apparently have unknown resistance mechanisms. On the other

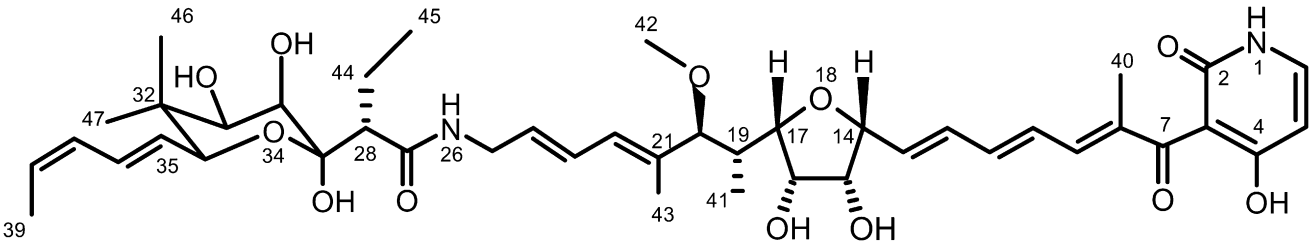

Figure 1. Chemical Structure of Kirromycin

hand, some producers of kirromycin-type antibiotics, like *S. cinnamoneus*, the producer of kirrothricin (Thein-Schranner et al., 1982), encode elongation factors that are resistant to their products (Olsthoorn-Tieleman et al., 2002).

The kirromycin molecule is a linear polyketide containing three intramolecular ring systems: the pyridone ring, the central tetrahydrofurane moiety, and a sugar-like structure named goldinonic acid (Figure 1). In feeding studies with the kirromycin-related compound aurodox (1-*N*-methyl-kirromycin) from *S. goldinensis* with isotope-labeled precursors, acetate was identified as the main building block of the carbon skeleton. These results indicate that the ethyl group at C-28 is derived from butyrate, the methyl group at C-8 from propionate, and the N-26 nitrogen from glycine. The other methyl groups, C-41, C-42, C-43, and C-46/C-47 originate from *S*-adenosyl-methionine. The biosynthetic origin of the pyridone ring, however, remained unclear because none of the provided substrates were incorporated into this part of the aurodox molecule (Liu et al., 1979).

The chemical structure and the observed acetate incorporation pattern indicate a polyketide biosynthesis mechanism involving hybrid type I polyketide synthases (PKSs) and nonribosomal peptide synthetases (NRPS). These modular enzymes have been studied in great detail (McDaniel et al., 2005; Staunton and Weissman, 2001). Type I PKSs are large, multifunctional megaenzymes catalyzing all steps required for polyketide synthesis. Each module of a classical type I PKS contains at least three distinct domains. In analogy to fatty acid biosynthesis, an acyltransferase (AT) domain loads the extender unit, usually malonyl-coenzyme A (CoA) or methylmalonyl-CoA, to the phosphopantetheinyl group of an acyl carrier protein (ACP) domain. A ketosynthase (KS) domain then catalyzes the condensation of the ACP-bound extender unit with the growing polyketide chain. Optionally, a set of domains (ketoreductase [KR], dehydratase [DH], and enoylreductase [ER] domains) is present that carries out reductions and dehydrations, respectively, on the β-keto group before the next chain elongation cycle takes place. This biosynthetic principle is observed in many antibiotic biosyntheses.

Hitherto, several variations of this mechanism have been discovered that illustrate the potential for structural diversity among microbial products. Complex polyketides, like pederin (Piel, 2002), the related compound, onnamide (Piel et al., 2004a), and bryostatin (Hildebrand et al., 2004), which are produced by yet-uncultivated bacterial symbionts of insects or marine sponges, leinamycin (Tang et al., 2004; Cheng et al., 2003), mupirocin (El Sayed et al., 2003), lankacidin (Arakawa et al., 2005), and some myxobacterial and fungal metabolites (Carvalho et al., 2005; Simunovic et al., 2006; Kim and Fuerst, 2006), are synthesized by PKSs that lack internal AT domains. In these cases, it is suggested that the loading of the PKS internal ACP domains is performed by external AT enzymes, which are present in biosynthetic gene clusters as individual enzymes. This hypothesis has been experimentally proven for the PKS that produces leinamycin (Cheng et al., 2003). To describe this architecture, the term "*trans*-AT PKS" has been introduced for enzymes lacking internal AT domains, whereas "*cis*-AT PKS" describes the "classical" AT-containing PKS.

Here we report the isolation, sequencing, and functional characterization of the kirromycin biosynthetic gene cluster, a novel member of the rare combined *cis*- and *trans*-AT PKS family and the molecular origin of the pyridone group of kirromycin.

RESULTS AND DISCUSSION

Isolation of the Kirromycin Biosynthetic Gene Cluster

A cosmid library of the kirromycin producer, *S. collinus* Tü 365, was generated with the cosmid vector, pOJ436 (Bierman et al., 1992). In total, 2304 clones were transferred into six 384-well plates and spotted onto hybridization membranes.

The chemical structure of kirromycin suggests a classical type I polyketide biosynthesis mechanism (PKS I). This knowledge can be exploited to construct primers for genetic screening (Weber et al., 2003). Degenerate primers were deduced from multiple sequence alignments of diverse *cis*-AT type clusters and used to label probes by PCR techniques. For the first screening, probes derived from other known PKS I producers (see Experimental Procedures) were labeled by using the primers KSII-FOR/ATIREV, and were subsequently pooled. We then generated a second DNA probe directly from the total DNA of the kirromycin producer, *S. collinus* Tü 365, by using the primers 1KS5′/2rAT3′.

In total, 43 hybridizing colonies were identified with the two probes. The cosmids were isolated and classified by restriction mapping (data not shown), resulting in four major families, along with seven cosmids that did not readily fit into these families.

In order to determine whether genes encoded on these cosmids are involved in kirromycin biosynthesis, one member of each family was subcloned with BamHI into the gene-inactivation vector, pK18mob/apra, and transferred into *S. collinus* Tü 365 via intergeneric conjugation. Mutant *S. collinus* 1C24, obtained after integration of p1C24u, which carries a 2.3 kb internal PKS fragment derived from cosmid 1C24, was no longer able to produce kirromycin (Figure 2). This result indicates that cosmid 1C24 carries genes of the kirromycin biosynthetic gene cluster.

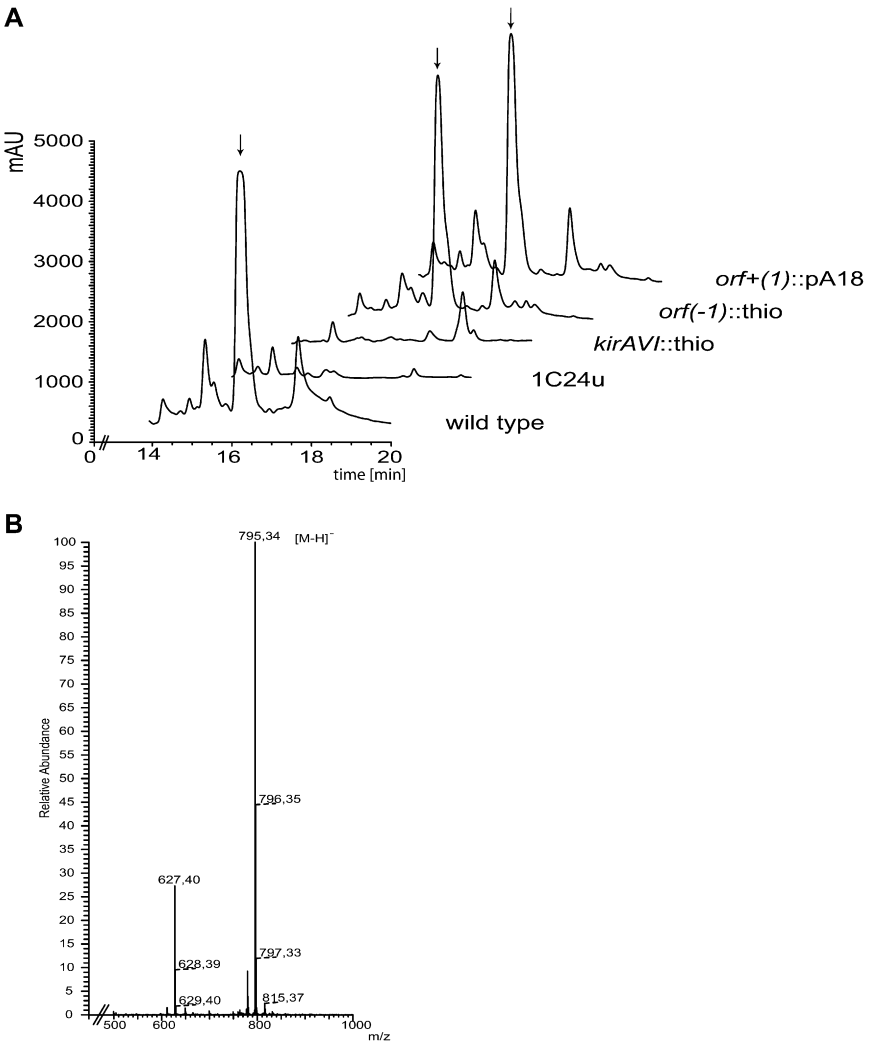

Figure 2. HPLC/MS Analyses of Mutants Generated in This Study

(A) HPLC-traces (UV detection at λ = 230–246 nm) of culture extracts of *S. collinus* Tü 365 wild type, and mutants 1C24u, *kirAVI*::thio, *orf(−1)*::thio, *orf(+1)*::pTLiNRPS2. Kirromycin (R_t = 16.5 min) was detected by UV-Vis (data not shown) and mass spectrometry.

(B) Mass spectrum of kirromycin, recorded in negative ion mode showing the characteristic *m/z* = 795 $[M-H]^-$Peak.

By subsequent screening with probes derived from the cosmid-insert ends, the four overlapping cosmids (6O07, 2C23, 1C24, and 2K05) were identified (Figure 3B).

Sequencing of the Kirromycin Biosynthesis Gene Cluster

Sequencing of the four identified cosmids covering 130 kb of the kirromycin biosynthesis locus resulted in the identification of 57 open reading frames (ORFs) (Figure 3). The overall GC content of the sequenced region is 73.7%. Approximately 60 kb code for eight enzymes related to polyketide biosynthesis. The region also contains nine genes with similarities to oxidoreductases, four putative regulatory genes, one methyltransferase gene, and some genes encoding hypothetical proteins. Surprisingly, a set of NRPS genes was also identified directly downstream of the putative kirromycin biosynthetic gene cluster. There are two DNA regions present in the sequenced region, spanning 1.36 and 1.88 kb, where no coding sequences were identified by automatic or manual analysis. For a full list of identified genes, see Table S1 in the Supplemental Data available with this article online.

Proof that the Isolated Genes Account for Kirromycin Biosynthesis

To ensure that the identified genes really encode the kirromycin biosynthesis gene cluster, a directed gene disruption of the PKS gene, *kirAVI*, was performed with the inactivation plasmid, pA18-*kirAVI*::thio. Among 576 clones that were tested for double crossover events, one clone was identified that was thiostrepton resistant and apramycin sensitive, and showed the correct fragment sizes in control PCR and Southern hybridization experiments (data not shown). This clone was termed *S. collinus kirAVI*::thio.

In bioassays against *S. albus* G, and in HPLC-MS-DAD analyses of extracts from culture supernatants, no kirromycin production was detected in this mutant (Figure 2). The loss of kirromycin production in the *S. collinus* mutants, 1C24 and *kirAVI*::thio, proves that the isolated genes are involved in kirromycin production and that we isolated the correct cluster.

Determination of the Cluster Boundaries

Apart from genes encoding PKS and typical secondary metabolite-related tailoring enzymes, several NRPS genes were identified that have no obvious function in kirromycin biosynthesis. Although the involvement of two NRPS modules can be postulated for the synthesis of the pyridone ring and the aliphatic amide bond, no distinct function of the remaining NRPS enzymes could be deduced from a hypothetical biosynthetic pathway. Most of the NRPS genes (*orf(+1), orf(+6)-(+8)*) are located in a cluster that is separated from the rest by a noncoding sequence gap containing 1881 bp. In order to test whether these peptide synthetases are involved in kirromycin biosynthesis, *orf(+1)* was disrupted with the inactivation plasmid, pA18-*orf(+1)*, resulting in mutant *orf(+1)*::pA18. The integration of this plasmid into the chromosome, which led to a loss of function of *orf(+1)*, was proven by Southern hybridization (data not shown). The mutation did not influence kirromycin production, as the antibiotic was still detectable by TLC and HPLC analyses of culture extracts (Figure 2). This indicates that *orf(+1)* is not involved in the

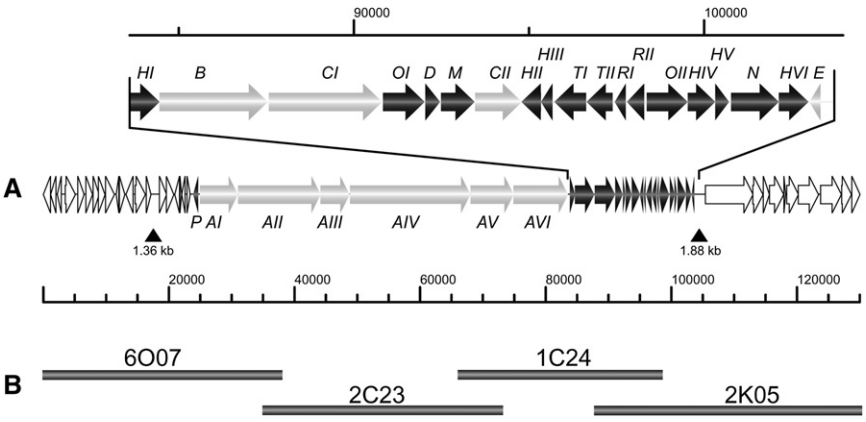

Figure 3. The Kirromycin Biosynthesis Gene Cluster

(A) Schematic representation of the kirromycin biosynthesis locus. White: genes putatively not involved in kirromycin biosynthesis; light gray: PKS and related genes; black: genes involved in tailoring reactions, precursor supply, regulation, transport, and with unknown function. The filled triangles indicate regions > 1 kb where no coding sequence was identified.

(B) Isolated and sequenced cosmids that overlap the kirromycin biosynthesis locus.

biosynthesis of kirromycin and, therefore, *orf(+1)* and the other genes identified in the NRPS region may code for the biosynthesis of a novel, yet unidentified, metabolite.

At the opposite site of the sequenced DNA region, *kirP* is, to our knowledge, the first gene for which we can postulate a putative function in kirromycin biosynthesis. *kirP* is located directly upstream from the first PKS gene, *kirAI*, in an inverse transcriptional orientation. Its gene product, KirP, is highly similar to Sfp-type phosphopantetheinyl transferases (66% similarity, 56% identity to PptA from the bleomycin producer, *S. verticillus*). These enzymes are usually required to attach a phosphopantetheine prosthetic group to carrier proteins of PKS and NRPS enzymes (Lambalot et al., 1996). To prove that KirP is involved in kirromycin biosynthesis, an inactivation plasmid was constructed by PCR amplification of the upstream and downstream DNA regions, followed by cloning into the conjugative vector pA18 and insertion of a thiostrepton resistance cassette derived from pSLE61 (Muth et al., 1988). This construct was introduced into *S. collinus*, where homologous recombination led to a disruption of *kirP* with the thiostrepton resistance gene which resulted in mutant *S. collinus kirP*::thio. The inactivation of *kirP* resulted in a significantly decreased level of antibiotic production (data not shown), indicating a role of *kirP* in kirromycin biosynthesis.

A similar gene inactivation experiment generated a mutant *orf(−1)*::thio to test whether the adjacent gene, *orf(−1)*, which encodes a highly conserved hypothetical protein, is also involved in the synthesis of kirromycin. The disruption of *orf(−1)* did not influence kirromycin production (Figure 2). Antibiotic production was still detectable by HPLC in culture extracts of mutant *orf(−1)*::thio. As all other upstream genes of *orf(−1)* have no homology to secondary metabolite biosynthesis genes, *orf(−1)* marks the upstream border region of the kirromycin biosynthesis gene cluster.

The results of the inactivation studies on *orf(−1)* and *orf(+1)* indicate that the kirromycin biosynthetic gene cluster comprises 26 genes spanning approximately 82 kb of DNA (Table 1).

Synthesis of the Kirromycin Backbone

The analysis of the PKS domain structure (Figure 4) indicates that the biosynthesis starts with the loading of acetyl-CoA to an unusual loading module of KirAI. This loading module consists of an N-terminal 320 aa-spanning domain (X_L) without sequence similarity to known proteins or conserved protein motifs and a typical ACP domain. There are a few indications that KirE, a putative GNAT-family acetyl transferase, might also be involved in loading the starter unit onto KirAI (see below). A prominent feature of kirromycin and its derivatives is the presence of a *cis*-olefinic structure at C-37 and C-38. Module 1 of KirAI does not contain a typical DH domain. Instead, the domain termed X_1 is present, which is weakly similar to a domain of unknown function in module 7 of the macrolactin PKS MlnE of *Bacillus amyloliquefaciens* FZB42 (Chen et al., 2007; Schneider et al., 2007) (23% identity, 38% similarity). Similar to kirromycin, no DH domain is encoded in this PKS module, but a *cis* double bond is present at the corresponding position in the macrolactin molecule. Thus, it is possible that the X_1 domain of KirAI and its homolog in MlnE are prototypes of novel DH domains catalyzing *cis* double-bond formations.

The polyketide chain is extended by the PKS modules of KirAI and KirAII, and then condensed with glycine by the hybrid NRPS/PKS KirAIII, which yields the amide bond and is further extended by the action of KirAIV-VI. The final step, a condensation of the kirromycin precursor with β-alanine, is proposed to be catalyzed by KirB. A thioesterase is neither present as a domain in PKS or NRPS enzymes, nor present as a separate enzyme in the gene cluster. This absence implies that the synthesized chain has to be cleaved, either driven by the pyridone ring formation from the PKS/NRPS complex or by an external thioesterase, which is recruited to cut off the product. Either during or after release, this intermediate has to undergo cyclization and oxidation to form the pyridone moiety (see below).

Interestingly, only the PKS KirAVI consists of the "classical" PKS domain organization: each of the two modules contains a KS, an AT, and an ACP domain. Module 14 also contains additional DH and KR domains. According to the hypothetical pathway and to the analysis of conserved amino acid positions in the active sites of the AT domains (Yadav et al., 2003), KirAVI adds two extender units to the nascent kirromycin precursor: one methylmalonyl-CoA and one malonyl-CoA, which are thought to build up a part of the pyridone moiety.

In contrast to the classical "*cis*-AT-type" organization of KirAVI, AT domains are absent in the other PKS modules. To our knowledge, kirromycin is the first actinomycete metabolite shown to be synthesized from combined *cis*- and *trans*-AT-type PKS I enzymes. Similar combinations of PKS types have

Table 1. Genes and Encoded Proteins Involved in Kirromycin Biosynthesis

Gene Name	aa/nt[a]	Putative Function	BLAST Score/ E Value	C/I[b]	Greatest Similarity to:	UniProt ID
orf(−1)	507/169	Hypothetical protein	269/2e−71	85.63/77.84	*Streptomyces avermitilis*	Q82IH7
kirP	756/252	Phosphopantetheinyl transferase	250/3e−65	66.11/56.49	*Streptomyces verticillus*	Q9F0Q6
kirAI	5982/1994	*Trans*-AT type PKS	1069/0.0	49.27/38.25	*Polyangium cellulosum*	Q2N3S9
kirAII	13152/4384	*Trans*-AT type PKS	1671/0.0	48.19/34.90	*Pseudomonas fluorescens* (strain Pf-5)	Q4KCD7
kirAIII	4653/1551	Hybrid NRPS/PKS	787/0.0	48.88/36.44	*Burkholderia pseudomallei*	Q63LK7
kirAIV	19197/6398	*Trans*-AT type PKS	1782/0.0	47.78/37.05	*Burkholderia thailandensis* (strain E264)	Q2T4P0
kirAV	6861/2287	*Trans*-AT type PKS	1005/0.0	49.28/37.17	*Sorangium cellulosum*	Q2N3S7
kirAVI	8697/2898	*Cis*-AT type PKS	2467/0.0	60.36/49.85	*Streptomyces halstedii*	Q0PCZ9
kirHI	849/283	Hypothetical protein	149/9e−35	49.63/36.03	*Streptomyces aureofaciens*	Q30CS4
kirB	3102/1034	Nonribosomal peptide synthase	535/1e−150	49.76/37.32	*Thermobifida fusca* (strain YX)	Q47NR9
kirCI	3237/1079	Acyltransferase	841/0.0	59.56/44.85	*Pseudomonas fluorescens*	Q8RL73
kirOI	1200/400	Cytochrome P450 hydroxylase	506/1e−142	83.93/74.40	*Frankia* sp. (strain CcI3)	Q2JE01
kirD	420/140	Aspartate 1-decarboxylase precursor	194/8e−49	83.82/72.06	*Frankia* sp. (strain CcI3)	Q2JE00
kirM	957/319	Methyltransferase	474/1e−132	85.53/73.90	*Streptomyces hygroscopicus*	Q54303
kirCII	1338/446	Acyltransferase	341/3e−92	60.39/47.19	*Stigmatella aurantiaca*	Q8RJY6
kirHII	558/186	Hypothetical protein	104/1e−21	52.63/40.35	*Streptomyces coelicolor*	Q9KYH5
kirHIII	333/111	Hypothetical protein	85.5/5e−16	62.39/44.95	*Streptomyces coelicolor*	Q9ZBI3
kirTI	903/301	Major facilitator superfamily transporter, *C*-terminus	261/2e−68	76.24/62.38	*Frankia sp.* (strain CcI3)	Q2JDZ4
kirTII	747/249	Major facilitator superfamily transporter, *N*-terminus	314/2e−84	81.74/66.96	*Frankia* sp. (strain CcI3)	Q2JDZ4
kirRI	315/105	Transcriptional regulatory protein, TetR family, *C*-terminus	107/1e−22	75.58/61.63	*Frankia* sp. (strain CcI3)	Q2JDZ6
kirRII	360/120	Transcriptional regulatory protein, TetR family, *N*-terminus	144/1e−33	86.27/67.65	*Frankia* sp. (strain CcI3)	Q2JDZ6
kirOII	1218/406	Cytochrome P450 hydroxylase	270/6e−71	58.11/41.62	*Streptomyces* sp. IHS-0435	Q595U8
kirHIV	783/261	Hypothetical protein	267/3e−70	67.45/54.12	*Frankia* sp. EAN1pec	Q3VY66
kirHV	396/131	Hypothetical protein	154/1e−36	76.27/64.41	*Frankia* sp. (strain CcI3)	Q2JDZ1
kirN	1368/456	Crotonyl CoA reductase	737/0.0	88.26/77.88	*Streptomyces collinus*	Q53865
kirHVI	846/282	Hypothetical protein	263/5e−69	67.63/50.00	*Burkholderia cepacia* (strain ATCC 17760)	Q39NX9
kirE	510/169	Acetyltransferase, GNAT family	72.0/8e−12	47.83/29.71	*Vibrio angustum* S14	Q1ZR07
orf(+1)	7392/2463	NRPS	1469/0.0	53.34/38.64	*Myxococcus xanthus* (strain DK 1622)	Q1D6B8

[a] aa, amino acids; nt, nucleotides.
[b] C, conserved amino acids in BLAST high-scoring sequence pairs; I, identical amino acids in BLAST high-scoring sequence pairs.

only been previously described for the biosynthesis of the myxobacterial metabolites chivosazol (Perlova et al., 2006) and myxovirescin A (Simunovic et al., 2006).

KirAI–KirAV have an unusual domain order and module organization. Normally, each PKS module starts with a KS and (in the case of *cis*-AT-type PKS) an AT domain, which are then

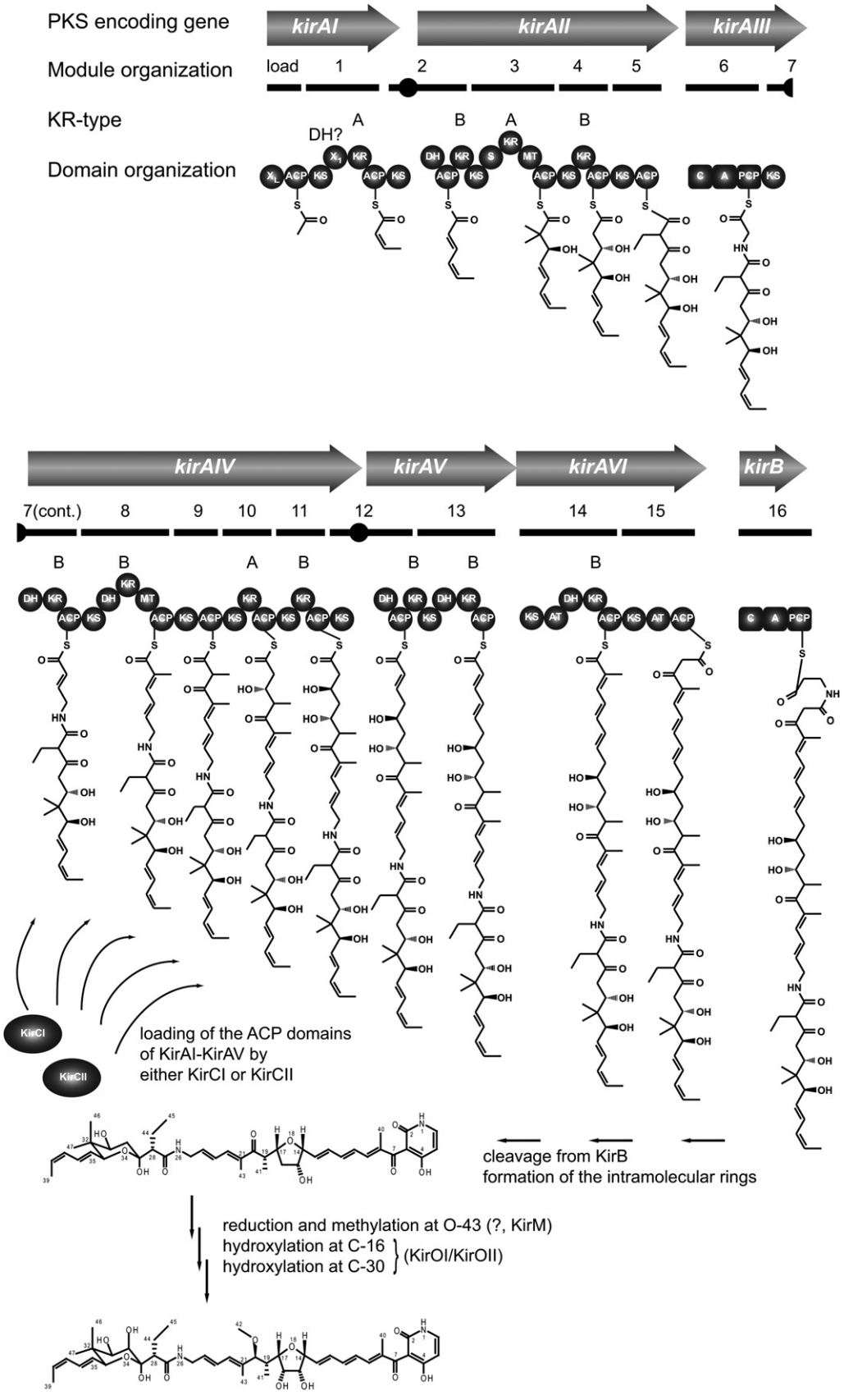
PKS encoding gene
kirAI
kirAII
kirAIII
Module organization
load
1
2
3
4
5
6
7
KR-type
A
B
A
B
DH?
Domain organization
kirAIV
kirAV
kirAVI
kirB
7(cont.)
8
9
10
11
12
13
14
15
16
KirCI
KirCII
loading of the ACP domains
of KirAI-KirAV by
either KirCI or KirCII
cleavage from KirB
formation of the intramolecular rings
reduction and methylation at O-43 (?, KirM)
hydroxylation at C-16
hydroxylation at C-30
(KirOI/KirOII)

alternatively followed by ER, DH, and KR domains. In most cases, the end of a module is determined by an ACP domain. However, the kirromycin PKS modules 2 and 12 show different organization. Instead of marking the end of the modules, both ACP domains are located between the DH and KR domains. Additionally, the KS domains of modules 2, 7, and 12 are not encoded on the same gene, but instead are located at the C terminus of the preceding PKS protein. To date, similar domain splitting had only been observed in other *trans*-AT-type PKS clusters, such as the biosynthetic gene clusters for leinamycin (Tang et al., 2004), pederin (Piel, 2002), chivosazol (Perlova et al., 2006), myxovirescin A (Simunovic et al., 2006), or macrolactin (Chen et al., 2007). These observations indicate that *trans*-AT PKS have more flexibility in their domain organization than *cis*-AT PKS.

The two methyl groups at position C-32 and the methyl groups at C-19 and C-21 are derived from *S*-adenosyl-methionine and not from propionate (Liu et al., 1979). This is consistent with the presence of methyltransferase domains in modules 3 and 8. Module 9 contributes to the incorporation of the C-17/C-19 acetate unit. No methyltransferase domain is present in this module, although the kirromycin molecule is methylated at the corresponding carbon C-19. There is no other enzyme with homology to C-methyltransferases present in the cluster. This apparent absence leads us to postulate that this methylation might be catalyzed by the methyltransferase domain of module 8 or by a methyltransferase not encoded in the kirromycin biosynthesis gene cluster. The KR domains present in the kirromycin cluster all show the proposed typical KR catalytic triad (Lys-Ser-Tyr, described by Reid et al. [2003]). Compared to *cis*-type PKS I, the DH domains present in KirAII, KirAIV, and KirAV are shorter than the DH domains from *cis*-AT-type PKS clusters. A similar observation was made in the leinamycin PKS (Tang et al., 2004). Again, some of the domains show variations in the consensus motif HxxxGxxxxP (according to Aparicio et al., 1996).

Putative Configurations and Ring Closures of Kirromycin Backbone Formation

The analysis of the central regions of the KR domains facilitates the prediction of the putative configuration of the resulting alcohols, or (with a subsequent action of a DH) of the resulting double bonds. KRs with the characteristic aspartate residue usually favor formation of D-configured alcohols (Reid et al., 2003). Correspondingly, additional action of DHs frequently leads to *trans* double bonds after ketoreductions (exceptions are known [Perlova et al., 2006]). In the case of kirromycin, the sequence data indeed predict the configurations of alcohols and double bonds as present in the kirromycin structure (Table S3). However, one has to consider that late biosynthetic steps, like oxygenations (C-30, C-16), furan ring formation (C14–C-17), or reduction/methylation (C-20-OCH_3), create new stereogenic centers in the kirromycin backbone.

Aside from the fully unsaturated pyridone ring, two additional intramolecular rings are characteristic of kirromycin in respect to other elfamycin congeners (for details on their putative biosynthesis see Supplemental Data). Presumably, the sugar-like goldinonic acid is formed via acetalization of the C-33 hydroxyl group (O-34) and the C-29 ketone as the chemically favored, six-membered pyran ring. While this usually spontaneous ring closure might already occur in the growing PKS chain (e.g., on module 5 of KirAII), hydroxylation of C-30 is likely accomplished by post-PKS oxygenation. Furan formation might be triggered by an initiatory dehydration of the PKS-derived C-15 hydroxyl group to give the double bond that is presumably epoxidized. Nucleophilic epoxide ring opening might furnish the C-14–C-17 furan ring, which is further oxidized (C-16-OH). However, the kirromycin sequence data do not support the presence of the necessary enzyme activities, such as DHs, epoxidases, or hydrolases (see Supplemental Data).

Two External AT Genes Are Encoded in the Kirromycin Biosynthesis Gene Cluster

kirCI and *kirCII* are two genes with products that are highly similar to ATs. They are encoded downstream of the PKS genes; *kirCI* encodes a 1078 aa protein, which has greatest similarity to MmpIII (44% identity, 59% similarity) from the mupirocin biosynthetic gene cluster from *Pseudomonas fluorescens* (El Sayed et al., 2003). This enzyme is believed to be responsible for the loading of the mupirocin PKS, which also lacks internal AT domains. Similar to MmpIII, KirCI contains two AT domains (KirCI_AT1 and KirCI_AT2) and an additional domain weakly homologous to oxidoreductases. While KirCI_AT2 shows a perfect match to the malonyl-CoA specificity amino acid signature (Yadav et al., 2003), two highly conserved amino acids are exchanged in KirCI_AT1. At position 91 (relating to *Escherichia coli* FabD amino acid numbering), a highly conserved histidine residue is replaced by alanine and, at position 117, a conserved arginine is exchanged for glutamine in KirCI. Interestingly, domain 1 of KirCI forms a distinct branch with domain 1 of MmpIII and PedC (pederin) (Figure S1). KirCI_AT2 clusters within a larger family containing LnmG (leinamycin) and domain 2 of MmpIII and PedD. This implies that the functions of PedC and PedD, which are encoded by two separate enzymes in pederin biosynthesis, might be provided by a single enzyme (KirCI) in kirromycin biosynthesis. In neither case has the specific function of these domains been experimentally determined.

The second enzyme, KirCII, contains only a single AT domain. In contrast to the AT domains of KirCI, this domain is a member of the methylmalonyl-CoA-specific family in phylogenetic analysis. This is also represented in the high similarity to the "classical" *cis*-type AT domain of the PKS StiA from the stigmatellin biosynthetic gene cluster (Gaitatzis et al., 2002) found in the myxobacterium, *Stigmatella aurantiaca*. The particular roles of KirCI and KirCII in kirromycin biosynthesis are currently under investigation. One of the ATs may be responsible for the loading of the ACP domains needed for the extension of the polyketide chain with malonyl-CoA, whereas the other may catalyze the loading of the single ethylmalonyl-CoA to the ACP domain of module 5.

Figure 4. Hypothetical Kirromycin Biosynthesis Pathway

A: adenylation domain; ACP: acyl carrier protein; AT: acyltransferase domain; C: condensation domain; DH: dehydratase domain ER: enoyl reductase domain; KR: keto reductase domain; KS: keto synthase domain; MT: methyl transferase domain; PCP: peptidyl carrier protein. X: Domains with unknown function. Modules that are split on two genes are indicated with a filled circle. KR type A leads to L configuration of the hydroxy group; KR type B leads to D configuration.

The gene product of *kirE* shows low similarity to *N*-acetyl transferases of the GNAT family (Interpro family: IPR000182). KirE shares 47% sequence similarity and 32% sequence identity to an as-yet uncharacterized putative acetyltransferase of *Solibacter usitatus* Ellin 6076. Notably, a GNAT domain is present in pederin biosynthesis as the first domain in the pederin PKS PedI. It is postulated that this domain plays an essential role in loading the acetyl-CoA starter unit to the ACP of the PKS loading module (Piel et al., 2004b). By analogy, KirE might also be involved in PKS priming.

The Origin of the Kirromycin Pyridone Moiety: Evidence from Feeding Experiments with ^{13}C-Labeled Precursors

Previous feeding studies on the related antibiotic aurodox did not reveal the biosynthetic origin of the pyridone group in kirromycin (Liu et al., 1979). In isotope feeding studies on the polyketide, efrotomycin, another member of the elfamycin family, it was shown that C-4 and C-5 of uracil are efficiently incorporated into the molecule (Darland et al., 1991). Hence, it was postulated, that the direct precursor might not be uracil, but rather the degradation product, β-alanine. While we did not find genes for uracil degradation in the cluster, the presence of KirD, a putative aspartate-1-decarboxylase, indicates aspartate as a different source for this building block in kirromycin biosynthesis.

The enzyme that is supposed to catalyze one of the key steps of pyridone biosynthesis is the NRPS KirB. Often, the specificity of these enzymes can be predicted by the analysis of specific amino acids of their adenylation domains. In the case of KirB, the signature of the specificity conferring amino acids present in KirB (DTLQLGVIWK) has not been observed before, so no good match against known motives described by Stachelhaus et al. (1999) and Challis et al. (2000) was found. Analysis by the machine learning-based method of Rausch et al. (2005) predicted a specificity against small amino acids, like alanine, valine, or amino butyric acid.

To test whether β-alanine is required for biosynthesis, feeding experiments with the kirromycin-producing *S. collinus* Tü 365 with ^{13}C-labeled putative precursors were performed. [1-^{13}C]acetate and [U-$^{13}C_3$ ^{15}N]β-alanine, respectively, were administered in aqueous solutions during the period of highest production between the 12th and 24th hour of fermentation. Kirromycin was isolated from the culture broth, yielding 6–7 mg l^{-1} of the pure compound, which was subjected to detailed ^{13}C-NMR analysis.

Feeding [1-^{13}C]acetate gave kirromycin with strongly labeled atoms. The labeling pattern corresponds with the predicted positions of acetate units as indicated (Table S2): C-24 showed no significant incorporation, which supports the speculation that C-24/C-25/N-26 originate from glycine. In contrast to aurodox biosynthesis (Liu et al., 1979), significant ^{13}C enrichment was detected, especially for the carbonyl C-2 atom of kirromycin from [1-^{13}C]acetate, which points to time-dependent labeling of the carboxylic acid pool of the cells during ^{13}C-feeding experiments. The putative butyrate unit (C-44, C-27), the propionate-derived C-7 atom, and the presumably β-alanine-derived C-4 atom are all significantly labeled in kirromycin, but not in aurodox. No incorporation was found in the methionine-derived carbon atoms. The ^{13}C-NMR spectrum of labeled kirromycin from [U-$^{13}C_3$ ^{15}N]β-alanine feeding showed complex coupling patterns due to strong ^{13}C-^{13}C and ^{13}C-^{15}N coupling. All acetate units were significantly double labeled, the propionate, butyrate, and glycine units showed labeling according to primary metabolism pathways, but not the methionine-derived atoms. Particularly high incorporation of [U-$^{13}C_3$ ^{15}N]β-alanine into the pyridone ring of kirromycin (C-4/C-5/C-6/N-1) was shown from the ^{13}C-NMR coupling pattern (Figure 5; Table S2). In addition, HR-ESI-mass spectrometry allowed for the determination of about 20% ^{15}N enrichment in the presence of additional ^{13}C-enriched isotopomers (Figure 5). Again, significant ^{13}C incorporation into the putative pyridone acetate unit (C-2/C-3) was determined from the coupling pattern in the pyridone ring. This result provides sound evidence that the pyridone moiety of kirromycin is built up with β-alanine. Release from KirB and cyclization of the pyridone ring may be driven by a nucleophilic attack at C-4 that is enabled by keto-enol tautomerism (for details see the Supplemental Data) as there is no thioesterase domain present in the cluster.

Precursor Supply

The two genes, *kirD* and *kirN*, both have high similarity to genes involved in primary metabolism. With 68% aa identity (80 % aa similarity), KirD shows high homology to PanD of *Streptomyces avermitilis*. PanD enzymes are aspartate-1-decarboxylases that are involved in the conversion of aspartate to β-alanine, a precursor of pantothenic acid. There are two putative functions for KirD in kirromycin biosynthesis. First, KirD may be involved in the "primary metabolism" function, which is the biosynthesis of phosphopantetheine. Phosphopantetheine is part of CoA and an essential cofactor of ACP and PCP domains in PKS and NRPS enzymes. A second possible role of KirD in antibiotic biosynthesis could be the formation of β-alanine as the last extender unit for the polyketide chain. So KirD would supply the kirromycin production machinery with this nonproteinogenic amino acid. The efficient incorporation of β-alanine into the pyridone group of kirromycin strongly favors this second function (see above).

KirN has 77% aa identity and 88% aa similarity to the previously characterized crotonyl-CoA reductase, Ccr, of *S. collinus* Tü 1892 (Wallace et al., 1995; Han and Reynolds, 1997). In this strain, which is different from the kirromycin producer, *S. collinus* Tü 365, the reduction of crotonyl-CoA to butyryl-CoA is part of an anaplerotic pathway that leads to formation of succinyl-CoA. Studies on aurodox (*N*-methyl kirromycin) indicate that the ethyl side chain is derived from butyrate (Liu et al., 1979). From this evidence, we assume that KirN is required to produce sufficient amounts of the precursor butyryl-CoA, which is subsequently carboxylated to ethylmalonyl-CoA. Similar enzymes have also been identified in the gene clusters of tylosin (Gandecha et al., 1997), concanamycin (Haydock et al., 2005), and other products that use PKS enzymes to incorporate ethylmalonyl-CoA.

Tailoring, Accessory, and Unknown Functions

After the kirromycin intermediate is released from KirB, some further post-PKS/NRPS biosynthetic steps are required to convert the intermediate into kirromycin.

According to the incorporation pattern of ^{13}C-labeled acetate and the functional assignment inferred from the analysis of the genome sequence, the hydroxy groups at C-16 and C-30 are not derived from malonyl-CoA incorporation during PKS

A

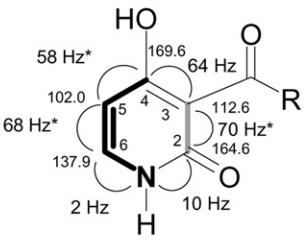

C-Atom	Chemical shift [ppm]	Specific Incorporation [%] Doublet	$J_{(C,C)}$ [Hz]	$J_{(C,N)}$ [Hz]
2	164.6	0.85	70,	(10)
3	112.6	0.41	70, (64)	n.d.
4	169.6	18.06	58*, (weak: 64)	n.d.
5	102.6	20.33	58*, 68*	n.d.
6	137.6	18.85	68*	2

B

[1-^{13}C]Acetate incorporation pattern

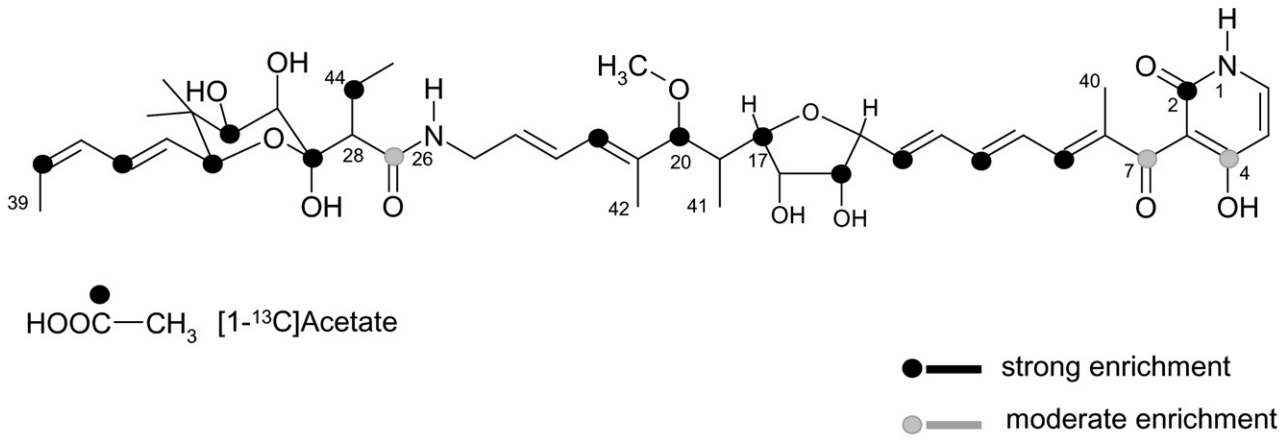

HOOC—CH_3 [1-^{13}C]Acetate

strong enrichment

moderate enrichment

[U-$^{13}C_3$ ^{15}N]-Alanine incorporation pattern

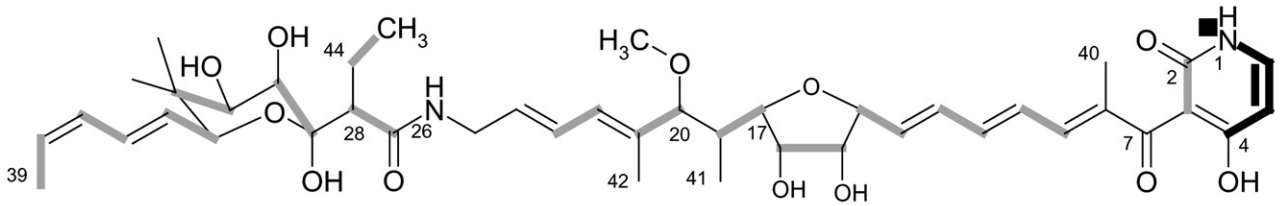

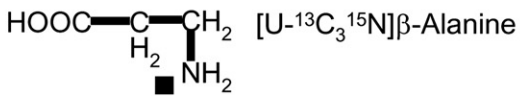

[U-$^{13}C_3$ ^{15}N]β-Alanine

Figure 5. ^{13}C NMR and Isotope Feeding Studies on Kirromycin

(A) Coupling constants from ^{13}C NMR spectra of the kirromycin pyridone fragment (150.8 MHz, CD_3OD) after feeding of [U-$^{13}C_3$ ^{15}N]β-alanine. Reference atom: Ø C-40, C-41, C-42, C-43, C-46, and C-47. Very strong coupling is indicated with an asterisk and very high enrichments by gray shading (Scott et al., 1974). Due to particularly high enrichment of the β-alanine unit, statistical coupling is observed for C-3/C-4.

(B) ^{13}C-incorporation patterns after feeding of *S. collinus* Tü 365 with isotope-labeled [1-^{13}C]acetate and [U-$^{13}C_3$ ^{15}N]β-alanine.

biosynthesis. Besides, tetrahydrofuran formation requires additional enzymatic steps.

KirOI and KirOII are two putative cytochrome P450-dependend hydroxylases encoded in the cluster that may be responsible for these steps. KirOI is highly similar (BLASTP: 44% identity, 59% similarity) to ORF4 of the mitomycin biosynthetic gene cluster of *S. lavendulae* (Mao et al., 1999). KirOII resembles P450 hydroxylases from *S. peucetius* (Parajuli et al., 2004) and EryF of

the erythromycin biosynthetic gene cluster of *Saccharopolyspora erythraea* (Andersen et al., 1993). Future mutational studies will provide further data to examine whether KirOI and KirOII are directly involved in the hydroxylations of C-16 and C-30 or whether they play a role in the formation of the tetrahydrofuran ring.

KirM is very similar to the *O*-methyltransferase RapM from the rapamycin biosynthesis gene cluster of *S. hygroscopicus* (73% identity, 85% similarity) (Chung et al., 2001). As there is only one *O*-methyl group at C-20, KirM might be involved in its formation. Unexpectedly, no KR domain is present in module 9, which would lead to generation of a hydroxy group that is the prerequisite for methyl transfer. While the absence of DH domains has been observed in other *trans*-AT-type PKS clusters, such as chivosazol (Perlova et al., 2006), leinamycin (Tang et al., 2004), or macrolactin (Schneider et al., 2007), the lack of KR domains has not, to our knowledge, been reported before. Thus, we have to postulate that the KR activity is provided by an as yet unidentified enzyme in *trans* or by an iterative usage of KR domains of adjacent modules 8 or 10 of the kirromycin PKS.

Six genes are encoded in the cluster, which share similarities with proteins of unknown function (KirHI–KirHVI). Their specific roles in the biosynthesis of kirromycin remain unclear. On the other hand, in the hypothetical biosynthetic pathway, there are some remaining steps that could not be attributed to any of the enzymes described above. These steps are (1) dehydrogenation toward the unsaturated pyridone ring, (2) the formation of C-20-OCH_3, (3) the formation of the intramolecular furan ring, and (4) the resistance of the producer.

Regulation and Transport

Only two ORFs in the kirromycin biosynthetic gene cluster encode proteins that are weakly similar to known regulatory proteins. In BLASTP analyses, the KirRI protein (104 aa) shows highest similarity to the C terminus of a putative, uncharacterized TetR family regulator (61% identity, 76% similarity) from *Frankia* sp. CcI3. The gene, *kirRII*, encoding a protein of 119 aa, is located directly upstream of *kirRI*. Its gene product is similar to the N-terminal half of the same *Frankia* protein. Whether KirRII and KirRI, which encode single proteins similar to the C- and N-terminal portions of different respective TetR repressors, combine to form a functional entity has yet to be experimentally proven.

A similar division into two proteins is observed in the KirTI and KirTII proteins, the genes of which are located directly downstream of *kirRI*. KirTI and KirTII are highly similar to the N- and C-terminal halves of *Frankia* sp. CcI3 and *S. coelicolor* major facilitator class export proteins. If these proteins are functional, they may be involved in kirromycin export and self-protection against the antibiotic.

SIGNIFICANCE

The structural features of kirromycin indicate the involvement of novel biosynthetic pathways. The analysis of the kirromycin biosynthesis gene cluster fully confirmed this assumption. The polyketide backbone of kirromycin is synthesized by a very unconventional hybrid nonribosomal peptide synthetase (NRPS)/polyketide synthase (PKS). The composition of these megaenzymes, which is unique among streptomycetes, shows a combination architecture of *cis*- and *trans*-AT-type PKS, variations of classical PKS domain organization, the occurrence of internal methyltransferase domains, and the presence of PKS domains with as yet unknown functions.

Predicted by sequence analysis of the gene cluster, the biosynthetic origin of the pyridone group of kirromycin could be proven experimentally by isotope feeding/NMR studies. To our knowledge, no similar pathway to pyridone formation has been described before on a molecular level.

The elucidation of the kirromycin biosynthesis gene cluster is a prerequisite to understanding the molecular principles of the biosynthesis of kirromycin-type antibiotics, and now enables the use of molecular techniques and/or combinatorial biosynthesis. It also opens new opportunities to study the molecular basics of natural product biosynthesis on enzymes that differ from classical PKS I model systems.

EXPERIMENTAL PROCEDURES

Strain Cultivation and General Methods

S. collinus Tü 365 was obtained from the "Tübinger Stammsammlung". For kirromycin production, the strain was cultivated in production medium consisting of soybean flour (10 g l^{-1}), mannite (10 g l^{-1}), $CaCO_3$ (5 g l^{-1}), and tap water. The pH was adjusted to 7.3 prior to sterilization. Cultivation for the isolation of spores was carried out on SFM (Kieser et al., 2000) or HA (malt extract [10 g l^{-1}], yeast extract [4 g l^{-1}], glucose [4 g l^{-1}], [pH 7.3]) agar. *E. coli* XL1-Blue was used as general cloning host for plasmid construction. Luria Bertani medium, supplemented with the appropriate antibiotics in their recommended concentrations, was used for *E. coli* propagation (Sambrook and Russell, 2001).

Methods for isolation and manipulation of DNA were performed as described by Sambrook and Russell (2001) and Kieser et al. (2000). Plasmid isolation was carried out with the QIAGEN Plasmid Mini/Midi Kit. DNA from agarose gels was isolated with QIAquick Kit or Amersham GFX columns. PCR amplifications were done with *Taq* DNA polymerase (QIAGEN). Restriction enzymes were purchased from New England Biolabs, MBI Fermentas, and Amersham, and used according to the suppliers' recommendations.

Extraction and Detection of Kirromycin

S. collinus wild-type or mutants were inoculated with a preculture (10%) in 100 ml of production broth and incubated for 3–5 days at 27°C/180 rpm in 500 ml shaking flasks. Culture supernatant was extracted twice with 1 volume ethyl acetate and concentrated completely in vacuo. The extract was then redissolved in appropriate volumes of MeOH (200 μl for 50 ml extraction volume).

Kirromycin production was assayed by TLC with silica gel 60 F_{254} plates (Merck), mobile phase: MeOH:$CHCl_3$ (1:10). Kirromycin was detected at wavelength λ = 254 nm and compared to purified substance (provided by H.P. Fiedler, Tübingen).

HPLC analyses were performed on an HP1090M/HP3392A/HP7994B system (Hewlett Packard) with Nucleosil C18 columns (5 μm, 125 mm × 4.6 mm) (Grom) with a flow rate of 2 ml min^{-1}. The following linear gradient for elution was applied using solvent PhoA (100% water with 0.1% phosphoric acid) and solvent AcCN (100% acetonitrile): at 0 min: 100% PhoA; at 15 min: 100%AcCN; at 16 min: PhoA, at 21 min: PhoA. Kirromycin was identified by comparison with purified substance or by comparison with an HPLC-UV/Vis spectra library (Fiedler, 1993).

Feeding Experiments, Isolation, and Chemical Analysis

A 150 ml sample of preculture of strain *S. collinus* Tü 365 (production medium, rotary shaker [BS4, Braun], 180 rpm, 30°C, 48 hr) in 1 l Erlenmeyer flasks (with three flow spoilers) was used to inoculate a 2 l fermentor vessel (Biostat B,

Braun) containing 900 ml of production medium. Standard fermentation conditions used were: 48 hr, 400 rpm, 4 vvm aeration, 30°C. Feeding experiments with [1-^{13}C]acetate (Amersham UK) and [$^{13}C_3$-^{15}N]β-alanine (Chemotrade) were carried out under conditions described above; precursors were administered to the fermentation as sterile aqueous solutions (40 ml). Continuous feeding with a low-rate pump (Ismatec) was carried out between the 12th and 24th hr of fermentation: Acetate feeding was as follows: [1-^{13}C]acetate (700 mg l^{-1}, 8.4 mmol l^{-1} culture broth). β-alanine feeding was as follows: [U-$^{13}C_3$^{15}N]β-alanine (250 mg l^{-1}, 2.7 mmol l^{-1} culture broth).

The culture broth was separated from the mycelium by filtration. The mycelium was discarded and the culture filtrate was extracted three times with equal amounts of ethyl acetate. The combined organic phases were evaporated to dryness and yielded the crude extracts (120 mg l^{-1}) that were reprecipitated in ethyl acetate and petroleum ether (1:8) (Brüning, 1996). The precipitate was applied for gel chromatography on Sephadex LH-20 (100 × 2.5 cm column, Pharmacia; eluent: methanol). All purification steps were monitored by TLC (0.25 mm silica gel 60 F_{254} plates [Merck]; anisaldehyde/sulfuric acid staining reagent: 1.0 ml of anisaldehyde in 85 ml MeOH, 5 ml of concentrated sulfuric acid, and 10 ml of acetic acid). The fractions containing kirromycin, as detected by TLC, were further purified by column chromatography on silica gel (Merck; $CHCl_3$:MeOH:methanol:25% NH_3, 8.0:2.0:0.5), and yielded pure kirromycin (acetate feeding, 6.7 mg; β-alanine feeding, 6.0 mg).

The presence of kirromycin in the extracts and its purity were monitored with HPLC-MS-DAD analysis (Flux Instruments Rheos 4000, Jasco 851-AS, Finnigan Surveyor, and LC-Q system) with a Superspher 100 RP-$18_{endc.}$ column (4 μm, 100 mm × 2 mm) (Grom) with a flow rate of 0.3 ml min^{-1}. The following linear gradient for elution was applied using solvents A (H_2O, 0.05% HCOOH) and B (MeOH, 0.05% HCOOH): at 0 min, 20% B; at 20 min, 100% B; at 25 min, 100% B; at 27 min, 20% B. Kirromycin was identified via MS ([M−H]: 795) and UV data (λ_{max} = 233 and 322 nm).

^{1}H-NMR and ^{13}C-NMR experiments on kirromycin from standard fermentations and feeding experiments were recorded in d_4-methanol (Varian Inova 600). Chemical shifts are expressed in δ values (ppm), with the solvent as internal reference, to allow for the detection of all signals due to overlapping or absence of different ^{13}C-NMR signals in other solvents (Barber et al., 1989). Specific incorporations were calculated according to established procedures (Scott et al., 1974). ^{13}C-NMR signals from nonlabeled and labeled kirromycin were normalized, and the specific incorporation calculated (specific incorporation = [1.1 × intensity of unlabeled signal/intensity of labeled signal − 1.1] × 100/enrichment of precursor. The specific incorporation of kirromycin from the [U-$^{13}C_3$^{15}N] β-alanine feeding experiment with ^{15}N was determined by HR-ESI-MS analysis (Bruker FTMS-7 APEX IV 70e FT-ICR spectrometer) by comparison with MS peaks of natural abundance: the MS peak of single ^{13}C label and single ^{15}N label showed a clear doublet with their respective intensities.

Generation of a Cosmid Library of *S. collinus* Tü 365

The genomic library of *S. collinus* Tü 365 was generated by using modified protocols from Beye et al. (1998) and Burgtorf et al. (1998). Homogenized mycelium was embedded in 0.5 % low melting point agarose (SeqPlaque GTG, Biozym), treated with 2 mg ml^{-1} lysozyme (Roth) for 14 hr at room temperature followed by 1 mg ml^{-1} Proteinase K (Merck) treatment for 24 hr at 50°C. The embedded DNA was partially digested with MboI, extracted with Gelase (Epicenter), and dephosphorylated. The resulting fragments were then ligated into 750 ng of BamHI-digested cosmid vector, pOJ436 (Bierman et al., 1992), desalted, packed (Gigapack III Gold Packaging Extract, Stratagene), and transferred into *E. coli* DH5α (Stratagene).

Screening of the Cosmid Library

Hybridizing probes were labeled nonradioactively with the Roche DIG PCR labeling kit. Primers used for probe labeling were:

(a) KSIIFOR: CTS GGS GAC CCS ATC GAG; ATIREV: GCS GCS GCG ATC TCS CCC TGS SWG TGS CC. Template DNA was obtained by genomic DNA preparation of *S. griseus* ssp. *sulphurus* Tü 1922, *S. antibioticus* Tü 99, *S. galbus* Tü 2253, *S. hygroscopicus* DSM 41530, *S. avermitilis* DSM 46492, *S. collinus* Tü 1892. The PCR program was: 94°C for 2 min; 30 cycles of 94°C for 1 min, 65°C for 1 min, and 72°C for 1 min; and 72°C for 5 min in an MJ Research PTC 225 thermocycler.

(b) 1KS5′: AGA ATT CGG SCC SGC SCT SAC SGT SGA CAC SGC S; 1rAT3′: TTT CTA GAS GCG ATC TCS CCC TGS GWG TGS CC. Template DNA was isolated from *S. collinus* Tü 365. The PCR program was: 94°C for 2 min; 30 cycles of 92°C for 1 min, 58°C for 1 min, 72°C for 2 min; 72°C for 5 min PCR using a Stratagene RoboCycler 40 Gradient yielded a 1.5 kb fragment was amplified.

The pooled PCR fragments and the 1.5 kb fragment obtained from the producing strain were DIG labeled and used as probes to screen the colony filters. Hybridization was performed under standard conditions.

Generation of PKS-Knockout Mutants

Cosmid DNA was isolated and digested with BamHI. Fragments with sizes of 1–4 kb were gel purified and cloned into pK18mob/apra (D. Schwartz, personal communication), a derivative of pK18mob with an apramycin resistance cassette introduced into the *aphII* promoter region. The plasmids were then transferred into *S. collinus* Tü 365 by intergeneric conjugation from *E. coli* ET12567 (Bierman et al., 1992) to the streptomycete. Kirromycin production was assayed via TLC/HPLC. For nonproducing mutants, correct integration of the plasmid was tested by PCR amplification of a 0.5 kb internal fragment of the introduced apramycin resistance gene (primer: apra-up: AGC TTC TCA ACC TTG G; apra-low: TCC GCC AAG GCA AAG C). The PCR program was: 94°C for 2 min; 30 cycles each of 94°C for 1 min, 50°C for 1 min, and 72°C for 1 min; and 72°C for 5 min on an MJ Research PTC100 thermocycler. The results of the PCR were confirmed by Southern hybridization that used the same PCR fragment labeled with Roche PCR-DIG labeling kit as a probe.

Generation of the *orf(+1)* Insertion Mutant *orf(+1)*::pA18

A 1.4 kb internal fragment of *orf(+1)* was amplified by PCR with the primers 1 dNRPS2-5′: AAG GTA CCA ATG CTG GAG GAC TAC G and 1 dNRPS2-3′: AGA AGC TTA GCC GGA GGT GTA GA, and cloned into vector pA18mob (pK18mob derivative, where *aphII* was totally replaced by the apramycin resistance cassette) via KpnI and HindIII. This resulted in the plasmid pA18-*orf(+1)*. Further procedures were identical to the generation of PKS-knockout mutants.

Generation of a *orf(−1)* Gene Replacement Mutant *orf(−1)*::thio

A 1.5 kb fragment of the flanking regions of *orf(−1)* was PCR amplified using the primers lorf-1_5′: GGA AGC TTG TCG GTG TTG TGC TTG GA/1orf-1_3′: GCT CTA GAC CTG GAA CCA GTG GTA CT and rorf-1_5′: AAG GTA CCA GGA GTA CGC CGA ACA GAG/rorf-1_3′: AAG AAT TCC GCG AGT CGA ATC TGG AG, resulting in the PCR products, lorf(−1) and rorf(−1). The following PCR program was applied in an MJ Research PTC100 thermocycler: 94°C for 2 min; 30 cycles each at 94°C for 1:15 min, 60°C for 1:30 min, and 72°C for 1:30 min; and 72°C for 5 min. The thiostrepton resistance cassette was obtained by XbaI/KpnI digestion of pSLE61 (Muth et al., 1988).

All PCR-fragments were individually cloned into the vector pDrive (QIAGEN). lorf(−1) was excised with KpnI and EcoRI, gel purified, and cloned into KpnI/EcoRI cut pA18. The right fragment was excised from pDrive with HindIII/XbaI and cloned into pA18 containing the left border fragment. To introduce the resistance marker, the plasmid containing both fragments was cut KpnI/XbaI and ligated with the thiostrepton resistance cassette, resulting in the plasmid pA18-*orf(−1)*::thio. Transfer to *S. collinus* wild type was performed as described above. Potential mutants were checked by PCR and Southern hybridization. To promote double crossover events, a stress protocol was applied: 400 μl of a spore suspension (~10^7 cells ml^{-1}) of clones carrying pA18-*orf(−1)*::thio in the genome were treated for 15 min in an ultrasonic bath, supplemented with 1 ml of TSB broth and incubated for 2 hr at 30°C. After the incubation, a second ultrasonic treatment (15 min) was applied. Subsequently, the spores were diluted and spread on HA agar plates containing thiostrepton (50 μg ml^{-1}). Clones where the double crossover had occurred were identified by replica plating on agar plates with thiostrepton (50 μg ml^{-1}) and thiostrepton/apramycin (each 50 μg ml^{-1}). Finally, the mutants were checked with PCR and Southern hybridization.

Generation of a *kirAVI* Gene Inactivation Mutant *kirAVI*::thio

Similar to the generation of the *orf(−1)* inactivation construct, flanking regions of *kirAVI* were amplified with the primers lkirAVI-hind-5′: ATA AGC TTC GGG CTC CGC GAT CTG AG/lkirAVI-kpn-3′: AAG GTA CCC ACC GCC TCC CAC GAG GTC and rkirAVI-kpn-5′ AAG GTA CCG TGT TCG TGG CCG AGT ACG G/rkirAVI-eco-3′: AAG AAT TCC CAC AGA GCG GTC TCC TTG C, resulting in PCR products lkirAVI and rkirAVI. The PCR fragments then were cloned into pDrive (QIAGEN). The thiostrepton resistance cassette was amplified with the primers thio-kpn-5′: AAG GTA CCG GCG AAT ACT TCA TAT GCG GGG AT/thio-kpn-3′: ACG GTA CCT CAC TGA CGA ATC GAG GTC GAG GA and also cloned into pDrive (QIAGEN) (for PCR program and equipment, see above).

The left fragment lkirAVI was cloned into pA18 by a HindIII/KpnI restriction/ligation. Subsequently, the right fragment was inserted via EcoRI/KpnI. Finally, the thiostrepton resistance cassette was cloned into the KpnI restriction site, resulting in plasmid pA18-*kirAVI*::thio. Transfer to *S. collinus* and generation and verification of the double crossover mutant was performed as described above.

Sequencing and Sequence Analysis

Shotgun sequencing of the cosmids was performed by GATC Biotech (Konstanz, Germany). The sequencing raw data were assembled with the software pipeline phred/phrap/consed (Ewing and Green, 1998; Ewing et al., 1998; Gordon et al., 1998). Automatic gene prediction was done with CRITICA (Badger and Olsen, 1999). Since the automatic gene identification process is error prone, manual control of the gene prediction was necessary, and was performed with the frame-plot tool provided by the program, ARTEMIS (Rutherford et al., 2000). Homologous sequences were identified with BLAST (Altschul et al., 1990), and protein motifs were identified with the software, HMMer (Eddy, 2004), searching the PFam database (Finn et al., 2006). Prediction of NRPS specificities was performed with the web application, NRPSpredictor, at http://www-ab.informatik.uni-tuebingen.de/software (Rausch et al., 2005).

ACCESSION NUMBERS

Coordinates have been deposited in the EMBL-nucleotide database under accession code AM746336.

SUPPLEMENTAL DATA

Supplemental Data, including three additional tables and one figure, are available online at http://www.chembiol.com/cgi/content/full/15/2/175/DC1/.

ACKNOWLEDGMENTS

We thank T. Härtner and D. Möckel for technical assistance and H.-P. Fiedler (University of Tübingen) for providing kirromycin and carrying out HPLC analyses. This work was funded by the Bundesministerium für Bildung und Forschung research grants 0313105 and 0313805 to W.W., T.W., S.G., and S.P. as part of the GenoMik and GenoMikPlus competence networks "Genome Research on Bacteria Relevant for Agriculture, Environment and Biotechnology." At the time this work was performed, K.W., A.V., and S.P. were employees of Combinature Biopharm AG, Berlin, Germany.

Received: June 29, 2007
Revised: November 27, 2007
Accepted: December 6, 2007
Published: February 22, 2008

REFERENCES

Alexander, C., Bilgin, N., Lindschau, C., Mesters, J.R., Kraal, B., Hilgenfeld, R., Erdmann, V.A., and Lippmann, C. (1995). Phosphorylation of elongation factor Tu prevents ternary complex formation. J. Biol. Chem. *270*, 14541–14547.

Altschul, S.F., Gish, W., Miller, W., Myers, E.W., and Lipman, D.J. (1990). Basic local alignment search tool. J. Mol. Biol. *215*, 403–410.

Andersen, J.F., Tatsuta, K., Gunji, H., Ishiyama, T., and Hutchinson, C.R. (1993). Substrate specificity of 6-deoxyerythronolide B hydroxylase, a bacterial cytochrome P450 of erythromycin A biosynthesis. Biochemistry *32*, 1905–1913.

Aparicio, J.F., Molnar, I., Schwecke, T., Konig, A., Haydock, S.F., Khaw, L.E., Staunton, J., and Leadlay, P.F. (1996). Organization of the biosynthetic gene cluster for rapamycin in *Streptomyces hygroscopicus*: analysis of the enzymatic domains in the modular polyketide synthase. Gene *169*, 9–16.

Arakawa, K., Sugino, F., Kodama, K., Ishii, T., and Kinashi, H. (2005). Cyclization mechanism for the synthesis of macrocyclic antibiotic lankacidin in *Streptomyces rochei*. Chem. Biol. *12*, 249–256.

Badger, J.H., and Olsen, G.J. (1999). CRITICA: coding region identification tool invoking comparative analysis. Mol. Biol. Evol. *16*, 512–524.

Barber, J., Derome, A.E., Howard, T.D., Lian, L., and Tebb, G. (1989). Full assignments of the ^{1}H and ^{13}C NMR spectra of the antibiotic kirromycin (mocimycin). Magn. Reson. Chem. *27*, 748–753.

Berger, J., Lehr, H., Teitel, S., Maehr, H., and Grunberg, E. (1973). A new antibiotic X-5108 of *Streptomyces* origin. I. Production, isolation and properties. J. Antibiot. (Tokyo) *26*, 15–22.

Beye, M., Poch, A., Burgtorf, C., Moritz, R.F., and Lehrach, H. (1998). A gridded genomic library of the honeybee (*Apis mellifera*): a reference library system for basic and comparative genetic studies of a hymenopteran genome. Genomics *49*, 317–320.

Bierman, M., Logan, R., O'Brien, K., Seno, E.T., Nagaraja-Rao, R., and Schoner, B.E. (1992). Plasmid cloning vectors for the conjugal transfer of DNA from *Escherichia coli* to *Streptomyces* spp. Gene *116*, 43–49.

Brüning, M. (1996). Diploma thesis. University of Göttingen, Göttingen, Germany.

Burgtorf, C., Welzel, K., Hasenbank, R., Zehetner, G., Weis, S., and Lehrach, H. (1998). Gridded genomic libraries of different chordate species: a reference library system for basic and comparative genetic studies of chordate genomes. Genomics *52*, 230–232.

Carter, G.T., Phillipson, D.W., Goodman, J.J., Dunne, T.S., and Borders, D.B. (1988). LL-E19020 alpha and beta, novel growth promoting agents: isolation, characterization and structures. J. Antibiot. (Tokyo) *41*, 1511–1514.

Carvalho, R., Reid, R., Viswanathan, N., Gramajo, H., and Julien, B. (2005). The biosynthetic genes for disorazoles, potent cytotoxic compounds that disrupt microtubule formation. Gene *359*, 91–98.

Challis, G.L., Ravel, J., and Townsend, C.A. (2000). Predictive, structure-based model of amino acid recognition by nonribosomal peptide synthetase adenylation domains. Chem. Biol. *7*, 211–224.

Chen, X.H., Koumoutsi, A., Scholz, R., Eisenreich, A., Schneider, K., Heinemeyer, I., Morgenstern, B., Voss, B., Hess, W.R., Reva, O., et al. (2007). Comparative analysis of the complete genome sequence of the plant growth-promoting bacterium *Bacillus amyloliquefaciens* FZB42. Nat. Biotechnol. *25*, 1007–1014.

Cheng, Y.Q., Tang, G.L., and Shen, B. (2003). Type I polyketide synthase requiring a discrete acyltransferase for polyketide biosynthesis. Proc. Natl. Acad. Sci. USA *100*, 3149–3154.

Chung, L., Liu, L., Patel, S., Carney, J.R., and Reeves, C.D. (2001). Deletion of *rapQONML* from the rapamycin gene cluster of *Streptomyces hygroscopicus* gives production of the 16-O-desmethyl-27-desmethoxy analog. J. Antibiot. (Tokyo) *54*, 250–256.

Clough, B., Rangachari, K., Strath, M., Preiser, P.R., and Wilson, R.J. (1999). Antibiotic inhibitors of organellar protein synthesis in *Plasmodium falciparum*. Protist *150*, 189–195.

Darland, G., Arison, B., and Kaplan, L. (1991). The biosynthetic origin of the pyridone ring of efrotomycin. J. Ind. Microbiol. *8*, 265–271.

Eddy, S.R. (2004). What is a hidden Markov model? Nat. Biotechnol. *22*, 1315–1316.

El Sayed, A.K., Hothersall, J., Cooper, S.M., Stephens, E., Simpson, T.J., and Thomas, C.M. (2003). Characterization of the mupirocin biosynthesis gene cluster from *Pseudomonas fluorescens* NCIMB 10586. Chem. Biol. *10*, 419–430.

Ewing, B., and Green, P. (1998). Base-calling of automated sequencer traces using phred. II. Error probabilities. Genome Res. *8*, 186–194.

Ewing, B., Hillier, L., Wendl, M.C., and Green, P. (1998). Base-calling of automated sequencer traces using phred. I. Accuracy assessment. Genome Res. *8*, 175–185.

Fiedler, H.-P. (1993). Biosynthetic capacities of actinomycetes: 1. Screening for secondary metabolite products by HPLC and UV-visible absorbance spectral libraries. Nat. Prod. Res. *2*, 119–128.

Finn, R.D., Mistry, J., Schuster-Bockler, B., Griffiths-Jones, S., Hollich, V., Lassmann, T., Moxon, S., Marshall, M., Khanna, A., Durbin, R., et al. (2006). Pfam: clans, web tools and services. Nucleic Acids Res. *34*, D247–D251.

Gaitatzis, N., Silakowski, B., Kunze, B., Nordsiek, G., Blöcker, H., Höfle, G., and Müller, R. (2002). The biosynthesis of the aromatic myxobacterial electron transport inhibitor stigmatellin is directed by a novel type of modular polyketide synthase. J. Biol. Chem. *277*, 13082–13090.

Gandecha, A.R., Large, S.L., and Cundliffe, E. (1997). Analysis of four tylosin biosynthetic genes from the *tylLM* region of the *Streptomyces fradiae* genome. Gene *184*, 197–203.

Gordon, D., Abajian, C., and Green, P. (1998). Consed: a graphical tool for sequence finishing. Genome Res. *8*, 195–202.

Hall, C.C., Watkins, J.D., and Georgopapadakou, N.H. (1989). Effects of elfamycins on elongation factor Tu from *Escherichia coli* and *Staphylococcus aureus*. Antimicrob. Agents Chemother. *33*, 322–325.

Han, L., and Reynolds, K.A. (1997). A novel alternate anaplerotic pathway to the glyoxylate cycle in streptomycetes. J. Bacteriol. *179*, 5157–5164.

Haydock, S.F., Appleyard, A.N., Mironenko, T., Lester, J., Scott, N., and Leadlay, P.F. (2005). Organization of the biosynthetic gene cluster for the macrolide concanamycin A in *Streptomyces neyagawaensis* ATCC 27449. Microbiology *151*, 3161–3169.

Hildebrand, M., Waggoner, L.E., Liu, H., Sudek, S., Allen, S., Anderson, C., Sherman, D.H., and Haygood, M. (2004). *bryA*: an unusual modular polyketide synthase gene from the uncultivated bacterial symbiont of the marine bryozoan *Bugula neritina*. Chem. Biol. *11*, 1543–1552.

Kieser, T., Bibb, M.J., Buttner, M.J., Chater, K.F., and Hopwood, D.A. (2000). Practical *Streptomyces* Genetics (Norwich: The John Innes Foundation).

Kim, T.K., and Fuerst, J.A. (2006). Diversity of polyketide synthase genes from bacteria associated with the marine sponge *Pseudoceratina clavata*: culture-dependent and culture-independent approaches. Environ. Microbiol. *8*, 1460–1470.

Lambalot, R.H., Gehring, A.M., Flugel, R.S., Zuber, P., LaCelle, M., Marahiel, M.A., Reid, R., Khosla, C., and Walsh, C.T. (1996). A new enzyme superfamily—the phosphopantetheinyl transferases. Chem. Biol. *3*, 923–936.

Liu, C.M., Williams, T.H., and Pitcher, R.G. (1979). ^{13}C-NMR studies on the biosynthesis of aurodox (antibiotic X-5108). J. Antibiot. (Tokyo) *32*, 414–417.

Maehr, H., Leach, M., Yarmchuk, L., and Stempel, A. (1973). Antibiotic X-5108. V. Structures of antibiotic X-5108 and mocimycin. J. Am. Chem. Soc. *95*, 8449–8450.

Mao, Y., Varoglu, M., and Sherman, D.H. (1999). Molecular characterization and analysis of the biosynthetic gene cluster for the antitumor antibiotic mitomycin C from *Streptomyces lavendulae* NRRL 2564. Chem. Biol. *6*, 251–263.

McDaniel, R., Welch, M., and Hutchinson, C.R. (2005). Genetic approaches to polyketide antibiotics. Chem. Rev. *105*, 543–558.

Mesters, J.R., Zeef, L.A., Hilgenfeld, R., de Graaf, J.M., Kraal, B., and Bosch, L. (1994). The structural and functional basis for the kirromycin resistance of mutant EF-Tu species in *Escherichia coli*. EMBO J. *13*, 4877–4885.

Muth, G., Wohlleben, W., and Pühler, A. (1988). The minimal replicon of the *Streptomyces ghanaensis* plasmid pSG5 identified by subcloning and Tn5 mutagenesis. Mol. Gen. Genet. *211*, 424–429.

Olsthoorn-Tieleman, L.N., Fischer, S.E., and Kraal, B. (2002). The unique *tuf2* gene from the kirromycin producer *Streptomyces ramocissimus* encodes a minor and kirromycin-sensitive elongation factor Tu. J. Bacteriol. *184*, 4211–4218.

Olsthoorn-Tieleman, L.N., Palstra, R.J., van Wezel, G.P., Bibb, M.J., and Pleij, C.W. (2007). Elongation factor Tu3 (EF-Tu3) from the kirromycin producer *Streptomyces ramocissimus* is resistant to three classes of EF-Tu-specific inhibitors. J. Bacteriol. *189*, 3581–3590.

Parajuli, N., Basnet, D.B., Chan, L.H., Sohng, J.K., and Liou, K. (2004). Genome analyses of *Streptomyces peucetius* ATCC 27952 for the identification and comparison of cytochrome P450 complement with other *Streptomyces*. Arch. Biochem. Biophys. *425*, 233–241.

Parmeggiani, A., and Swart, G.W.M. (1985). Mechanism of action of kirromycin-like antibiotics. Annu. Rev. Microbiol. *39*, 557–577.

Perlova, O., Gerth, K., Kaiser, O., Hans, A., and Müller, R. (2006). Identification and analysis of the chivosazol biosynthetic gene cluster from the myxobacterial model strain *Sorangium cellulosum* So ce56. J. Biotechnol. *121*, 174–191.

Piel, J. (2002). A polyketide synthase-peptide synthetase gene cluster from an uncultured bacterial symbiont of *Paederus* beetles. Proc. Natl. Acad. Sci. USA *99*, 14002–14007.

Piel, J., Hui, D., Wen, G., Butzke, D., Platzer, M., Fusetani, N., and Matsunaga, S. (2004a). Antitumor polyketide biosynthesis by an uncultivated bacterial symbiont of the marine sponge *Theonella swinhoei*. Proc. Natl. Acad. Sci. USA *101*, 16222–16227.

Piel, J., Wen, G., Platzer, M., and Hui, D. (2004b). Unprecedented diversity of catalytic domains in the first four modules of the putative pederin polyketide synthase. Chembiochem *5*, 93–98.

Rausch, C., Weber, T., Kohlbacher, O., Wohlleben, W., and Huson, D.H. (2005). Specificity prediction of adenylation domains in nonribosomal peptide synthetases (NRPS) using transductive support vector machines (TSVMs). Nucleic Acids Res. *33*, 5799–5808.

Reid, R., Piagentini, M., Rodriguez, E., Ashley, G., Viswanathan, N., Carney, J., Santi, D.V., Hutchinson, C.R., and McDaniel, R. (2003). A model of structure and catalysis for ketoreductase domains in modular polyketide synthases. Biochemistry *42*, 72–79.

Rutherford, K., Parkhill, J., Crook, J., Horsnell, T., Rice, P., Rajandream, M.A., and Barrell, B. (2000). Artemis: sequence visualization and annotation. Bioinformatics *16*, 944–945.

Sambrook, J., and Russell, D.W. (2001). Molecular Cloning: A Laboratory Manual, Third Edition (Cold Spring Harbor, NY: Cold Spring Harbor Laboratory Press).

Schmid, B., Anke, T., and Wolf, H. (1978). Action of pulvomycin and kirromycin on eukaryotic cells. FEBS Lett. *96*, 189–191.

Schneider, K., Chen, X.H., Vater, J., Franke, P., Nicholson, G., Borriss, R., and Süssmuth, R.D. (2007). Macrolactin is the polyketide biosynthesis product of the *pks2* cluster of *Bacillus amyloliquefaciens* FZB42. J. Nat. Prod. *70*, 1417–1423.

Scott, A.I., Townsend, C.A., Okada, K., Kajiwara, M., Cushley, R.J., and Whitman, P.J. (1974). Biosynthesis of corrins. II. Incorporation of ^{13}C-labeled substrate in vitamins B_{12}. J. Am. Chem. Soc. *96*, 8069–8080.

Simunovic, V., Zapp, J., Rachid, S., Krug, D., Meiser, P., and Müller, R. (2006). Myxovirescin A biosynthesis is directed by hybrid polyketide synthases/nonribosomal peptide synthetase, 3-hydroxy-3-methylglutaryl-CoA synthases, and *trans*-acting acyltransferases. ChemBioChem *7*, 1206–1220.

Stachelhaus, T., Mootz, H.D., and Marahiel, M.A. (1999). The specificity-conferring code of adenylation domains in nonribosomal peptide synthetases. Chem. Biol. *6*, 493–505.

Staunton, J., and Weissman, K.J. (2001). Polyketide biosynthesis: a millennium review. Nat. Prod. Rep. *18*, 380–416.

Tang, G.L., Cheng, Y.-Q., and Shen, B. (2004). Leinamycin biosynthesis revealing unprecedented architectural complexity for a hybrid polyketide synthase and nonribosomal peptide synthetase. Chem. Biol. *11*, 33–45.

Tavecchia, P., Marazzi, A., Dallanoce, C., Trani, A., Ciciliato, I., Ferrari, P., Selva, E., and Ciabatti, R. (1996). Synthesis and biological evaluation of new fragments from kirromycin antibiotic. J. Antibiot. (Tokyo) *49*, 1249–1257.

Thein-Schranner, I., Zähner, H., Hoppe, H.U., Hummel, I., and Zeeck, A. (1982). Metabolic products of microorganisms. 209 Kirrothricin, a new member of the kirromycin-group. J. Antibiot. (Tokyo) *35*, 948–956.

Vogeley, L., Palm, G.J., Mesters, J.R., and Hilgenfeld, R. (2001). Conformational change of elongation factor Tu (EF-Tu) induced by antibiotic binding. Crystal structure of the complex between EF-Tu.GDP and aurodox. J. Biol. Chem. *276*, 17149–17155.

Vos, C., and Verwiel, P.E.J. (1973). The total structure of the novel antibiotic mocimycin (MYC 8003). Tetrahedron Lett. *14*, 5173–5176.

Wallace, K.K., Bao, Z.Y., Dai, H., Digate, R., Schuler, G., Speedie, M.K., and Reynolds, K.A. (1995). Purification of crotonyl-CoA reductase from *Streptomyces collinus* and cloning, sequencing and expression of the corresponding gene in *Escherichia coli*. Eur. J. Biochem. *233*, 954–962.

Wax, R., Maises, W., Weston, R., and Birnbaum, J. (1976). Efrotomycin, a new antibiotic from *Streptomyces lactamdurans*. J. Antibiot. (Tokyo) *29*, 670–673.

Weber, T., Welzel, K., Pelzer, S., Vente, A., and Wohlleben, W. (2003). Exploiting the genetic potential of polyketide producing streptomycetes. J. Biotechnol. *106*, 221–232.

Wolf, H., and Zähner, H. (1972). Metabolic products of microorganisms. 99. Kirromycin. Arch. Mikrobiol. *83*, 147–154, [Article in German].

Wolf, H., Gianni, C., and Parmeggiani, A. (1972). Metabolic products of microorganisms. 100. Kirromycin, an inhibitor of 30S ribosomal subunit function. FEBS Lett. *21*, 347–350.

Wolf, H., Chinali, G., and Parmeggiani, A. (1974). Kirromycin, an inhibitor of protein biosynthesis that acts on elongation factor Tu. Proc. Natl. Acad. Sci. USA *71*, 4910–4914.

Yadav, G., Gokhale, R.S., and Mohanty, D. (2003). Computational approach for prediction of domain organization and substrate specificity of modular polyketide synthases. J. Mol. Biol. *328*, 335–363.

Zimmerman, S.B., Chalmers, J.H., Jr., Dewey, R.S., Stapley, E.O., and Hernandez, S. (1979). Heneicomycin, a new antibiotic (A21A): fermentation, isolation, and antibacterial spectrum. J. Antibiot. (Tokyo) *32*, 665–666.

